Received: 3 December 2019

DOI: 10.1002/asna.202013730

Astronomische Nachrichten

ORIGINAL ARTICLE

Flickering of the jet-ejecting symbiotic star MWC 560

R. K. Zamanov | S. Boeva | K. A. Stoyanov | G. Latev | B. Spassov | A. Kurtenkov | G. Nikolov

Institute of Astronomy and National Astronomical Observatory, Bulgarian Academy of Sciences, Sofia, Bulgaria

Correspondence
R. K. Zamanov, Institute of Astronomy and National Astronomical Observatory, Bulgarian Academy of Sciences, Tsarigradsko Shose 72, BG-1784 Sofia, Bulgaria.
Email: rkz@astro.bas.bg

Funding information
Bulgarian National Science Fund, Grant/Award Number: KP-6-H28/2

Abstract

We analyzed the optical photometric data of short-term variability (flickering) of the accreting white dwarf in the jet-ejecting symbiotic star MWC 560. The observations were obtained on 17 nights during the period November 2011 to October 2019. The color-magnitude diagram shows that the hot component of the system becomes redder as it gets brighter. For the flickering source, we find that it has color $0.14 < B - V < 0.40$, temperature in the range $6{,}300 < T_{fl} < 11{,}000$ K, and radius $1.2 < R_{fl} < 18\ R_{\odot}$. We find a strong correlation (correlation coefficient 0.76, significance <0.001) between B band magnitude and the average radius of the flickering source—as the brightness of the system increases, the size of the flickering source also increases. The estimated temperature is similar to that of the bright spot of cataclysmic variables. In 2019, the flickering was missing, and the B–V color of the hot component became bluer.

KEYWORD

accretion, accretion discs – (stars:) novae, cataclysmic variables – binaries: symbiotic – stars: individual: MWC 560

1 | INTRODUCTION

Symbiotic stars are wide binaries with long orbital periods (from 100 days to 100 years) in which material is transferred from an evolved red giant star to a white dwarf or a neutron star (Mikołajewska 2012). The symbiotic star MWC 560 (V694 Mon) was identified as an emission line object in the Mount Wilson observatory spectroscopic surveys (Merrill & Burwell 1943). The spectroscopic observations of MWC 560 in 1984 showed that it is an extraordinary symbiotic star with absorption extending to $-3{,}000\ \mathrm{km\,s^{-1}}$ at Hβ and higher members of the Balmer series (Bond et al. 1984). In early 1990, the outflow velocities reached 6,000–7,000 $\mathrm{km\,s^{-1}}$ (Szkody et al. 1990; Tomov et al. 1990). Tomov et al. (1990) proposed that the observed absorptions are caused by a collimated outflow along the line of sight—a low-energy analog of the jets of the microquasar SS 433. The outflow may be a highly collimated baryon-loaded jet (Schmid et al. 2001) or a wind from the polar regions (Lucy et al. 2018). MWC 560 is considered to be a nonrelativistic analog of the quasars not only because of its jets but also because of the resemblance of its emission lines to that of the low-redshift quasars (Zamanov & Marziani 2002) and the absorption lines to that of the broad absorption lines quasars (Lucy et al. 2018). The orbital period of the binary is thought to be $P_{\mathrm{orb}} = 1{,}931 \pm 162$ d (Gromadzki et al. 2007), although recently, Munari et al. (2016) supposed that it could be considerably shorter, $P_{\mathrm{orb}} \approx 330.8$ d.

Systematic searches for flickering variability in symbiotic stars and related objects (Angeloni et al. 2013; Dobrzycka et al. 1996; Gromadzki et al. 2006; Sokoloski et al. 2001) have shown that optical flickering is a rarely detectable phenomenon in symbiotic stars. Among more than 200 symbiotic stars known, only in 11 objects is flickering activity visible. A flickering variability of MWC 560 of

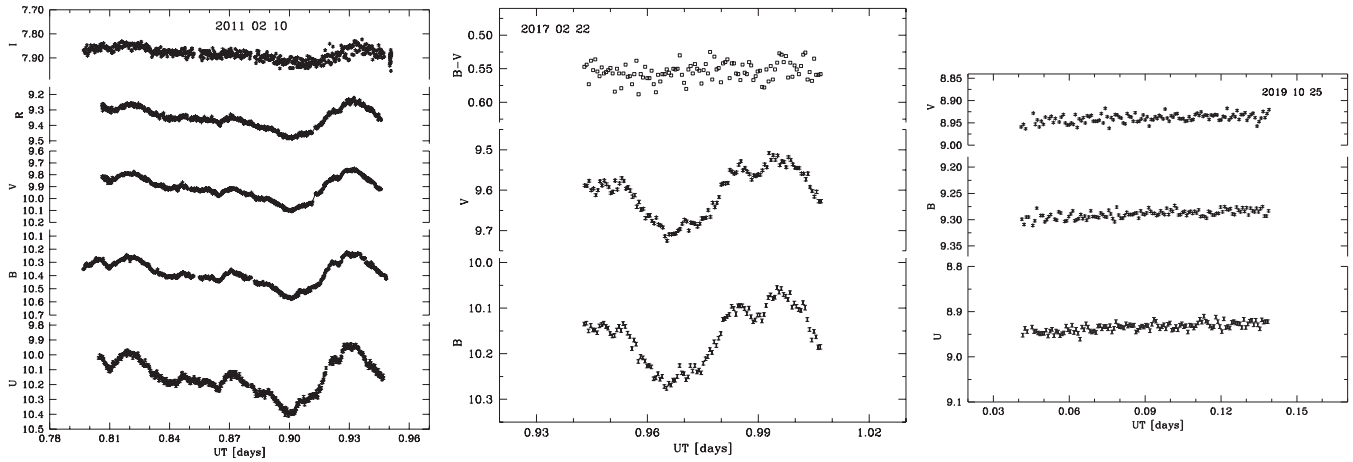

FIGURE 1 Examples of the short-term variability of MWC 560. The label in each panel indicate the date of observations in the format YYYYMMDD. The left panel is 20110210—UBVRI data (the flickering is visible even in I-band, and its amplitude is decreasing to the red bands). The middle panel is 20170222—the light curves in B- and V-bands together with the calculated B–V color. The right panel is 20191025—UBV data, and the flickering is missing

up to 0.2 mag on a timescale of a few minutes was first reported by Bond et al. (1984). The amplitude is in the range 0.1–0.7 mag, and the detected quasiperiods are from 11 to 160 min (Tomov et al. 1996). The intranight variability was a persistent feature till 2018, when the variability on the timescale of minutes became undetectable (Goranskij et al. 2018).

Here, we report quasisimultaneous observations of the flickering variability of the jet-ejecting symbiotic star MWC 560 (most of them in the two optical bands—B and V) and analyze the color changes, temperature, and radius of the flickering source and their response to the brightness variations.

2 | OBSERVATIONS AND DATA ANALYSIS

The observations were performed with four telescopes equipped with charge-coupled device (CCD) cameras:

1. the 2.0-m telescope of the National Astronomical Observatory (NAO) Rozhen, Bulgaria (Bonev & Dimitrov 2010)
2. the 50-/70-cm Schmidt telescope of NAO Rozhen
3. the 60-cm telescope of NAO Rozhen
4. the 60-cm telescope of the Belogradchik Observatory, Bulgaria (Strigachev & Bachev 2011)

Data reduction was carried out with IRAF (Tody 1993) following standard recipes for the processing of CCD images and aperture photometry. A few comparison stars from the list of Henden & Munari (2006) and APASS DR9 have been used. The typical photometric errors are 0.007 mag in U-band, 0.005 mag in B-band, and 0.004 mag in V-band.

Three examples of our data are given in Figure 1. In the left panel (20110210), UBVRI data are plotted. The amplitude in U-band is 0.47 mag, in B-band is 0.34 mag, in V-band is 0.32 mag, in R-band is 0.23 mag, and in I-band is 0.07 mag. The amplitude of the flickering decreases to longer wavelengths, mainly due to the increasing contribution of the red giant, which is the dominating source in infrared bands. In the middle panel (20170222), the light curves of MWC 560 in B- and V-bands are plotted together with the calculated B–V color. The right panel demonstrates UBV data obtained on 20191025 when the flickering is missing. If it exists at all, its amplitude in UBV is <0.02 mag.

We assess 17 nights with simultaneous observations in B- and V-bands during the period July 2008 to October 2019. The $B–V$ color is calculated for a total of 2,307 points. During our observations, the brightness of MWC 560 was:

$$9.20 \leq B \leq 11.92,$$

$$8.60 \leq V \leq 11.33,$$

$$0.31 \leq B - V \leq 0.67,$$

with mean B = 10.28, mean V = 9.81, and mean B–V = 0.47. When the flickering exists, its peak-to-peak amplitude in the B-band is in the range 0.13–0.39 mag.

The journal of observations is given in Table 1. Table 2 demonstrates the number of data points over which B–V color is calculated along with the average, minimum, and maximum magnitudes in B- and V-bands.

TABLE 1 Journal of observations

Date YYYYMMDD	Telescope	Bands	UT start–UT-end	Detection
20091114	2.0 Roz	U	23:59–01:27	Yes
	50/70 Sch	B	00:21–01:32	Yes
	60 Bel	V	00:22–01:27	Yes
	60 Roz	R	00:14–01:34	Yes
20100111	2.0 Roz	U, V	23:31–01:04	Yes
	50/70 Sch	B	23:28–01:10	Yes
	60 Roz	R, I	23:13–01:01	Yes
20100315	60 Roz	V, I	18:00–19:15	Yes
20100317	60 Roz	V, I	18:08–19:14	Yes
20101229	2.0 Roz	U	22:55–01:28	Yes
	60 Bel	V, R	22:10–01:30	Yes
	60 Roz	B, I	21:53–01:31	Yes
20110210	2.0 Roz	U	19:18–22:43	Yes
	60 Roz	B, I	19:07–22:45	Yes
	60 Bel	V, R	19:20–22:41	Yes
20110211	60 Roz	U, B	19:35–22:59	Yes
	60 Bel	V, R, I	19:34–23:01	Yes
20110212	60 Roz	U, B, V, R, I	20:25–22:47	Yes
20120321	60 Bel	B, V, R	18:27–20:20	Yes
20120323	60 Bel	B, V, R, I	18:06–20:15	Yes
20130303	60 Bel	B, V, R, I	19:35–21:10	Yes
20130305	60 Bel	B, V, R, I	18:37–20:31	Yes
20131129	60 Roz	B, V, R, I	00:26–03:31	Yes
20151118	60 Bel	B, V, R, I	02:10–04:19	Yes
20160402	60 Bel	B, V	18:12–19:25	Yes
20160405	50/70 Sch	B	17:40–19:11	Yes
20170222	60 Bel	B, V	22:37–00:09	Yes
20180124	50/70 Sch	B, V, R, I	22:18–22:50	Yes
20191022	50/70 Sch	B, V	00:17–03:49	No
20191025	50/70 Sch	U, B, V	00:59–03:19	No
20200201	50/70 Sch	B	19:50–21:15	No

Note: In the table are given the dates of observations, the telescope, the filter, UT start and end of the run, and detection/nondetection of flickering.

3 | PARAMETERS OF THE SYSTEM

GAIA DR2 (Gaia Collaboration et al. 2018) gives 0.3534 ± 0.1659 for the MWC560 parallax, which corresponds to a distance d = 2830 pc. Schmid et al. (2001) derived distance 2.5 ± 0.7 kpc, which agrees with the GAIA value.

Schmid et al. (2001) estimated interstellar extinction E(B–V) = 0.15 mag from the 2,200 Å feature and for the mass donor spectral type M5.5 III. Slightly different values were found earlier by Zhekov et al. (1996)—M4.5 III and E(B–V) = 0.23 mag. The extinction is most likely in the range $0.1 \leq E(B-V) \leq 0.2$ in the light of the NaD absorption and dust maps (Lucy et al. 2020). Houdashelt et al. (2001) find, for M5.5 III, giant colors, B–V = 1.55 and V–I = 2.7.

For the red giant, Zhekov et al. (1996) estimated $m_B \sim 14$ mag, which is in agreement with the long-term

TABLE 2 Data used to calculate the B–V color of MWC 560

Date		Mean(B)	Min(B)	Max(B)	Mean(V)	Min(V)	Max(V)
YYYYMMDD	N_{pts}	[mag]	[mag]	[mag]	[mag]	[mag]	[mag]
20091114	39	11.8557	11.799	11.921	11.2766	11.240	11.329
20100111	52	11.5749	11.410	11.715	11.0412	10.894	11.163
20101229	360	10.1520	10.040	10.245	9.6801	9.587	9.778
20110210	477	10.3856	10.224	10.580	9.9110	9.747	10.108
20110211	186	10.4426	10.331	10.568	9.9949	9.899	10.116
20110212	143	10.3205	10.205	10.460	9.8805	9.776	10.018
20120321	70	10.6389	10.496	10.752	10.1055	9.9440	10.205
20120323	93	10.9392	10.776	11.079	10.4181	10.227	10.577
20130303	100	10.8227	10.755	10.888	10.3261	10.247	10.394
20130305	79	11.0507	10.880	11.191	10.5484	10.385	10.662
20131129	75	10.9839	10.764	11.134	10.5579	10.331	10.696
20151118	87	10.1774	10.032	10.420	9.6246	9.481	9.813
20160402	88	9.3861	9.202	9.535	8.7897	8.605	8.953
20170222	110	10.1601	10.055	10.276	9.6060	9.508	9.725
20180124	27	10.2431	10.134	10.299	9.8144	9.716	9.868
20191022	207	9.2703	9.254	9.293	8.9272	8.909	8.950
20191025	114	9.2885	9.273	9.311	8.9387	8.917	8.967

Note: In the table are given the date, N_{pts} (the number of data points over which B–V color is calculated), average, and minimum and maximum magnitudes in B- and V-bands.

light curve of MWC 560 (Doroshenko et al. 1993). With the above color and extinction, this gives, for the red giant, $m_V \sim 12.30$ mag. Using J- and K-band data from 2MASS All Sky Catalog (J = 6.452, K = 5.069) and the extinction law from Savage & Mathis (1979), we obtain $A_J = 0.13$ and $A_K = 0.06$. Koornneef (1983) gives intrinsic colors V–K = 6.7 and V–J = 5.43 for an M5.5 III star. Using these parameters, we derive $m_V = 12.23$ and $m_V = 12.19$ using J- and K-bands, respectively.

Hereafter, we assume, for the red giant component of MWC 560, $m_V \approx 12.25$ and $m_B \approx 13.94$. These magnitudes are used in Section 4 to estimate the colors of the hot component.

4 | VARIABILITY IN B- AND V-BANDS

In Figure 2, we plot B- versus V-band magnitude. The left panel (Figure 2a) demonstrates the observed magnitudes of MWC 560. The right panel (Figure 2b) demonstrates the dereddened magnitudes of the hot component (e.g., the red giant contribution is subtracted using the magnitudes given in Section 3).

In Figure 3, we plot color-magnitude diagrams. The color-magnitude diagram is quite different from that of the cataclysmic variable AE Aqr (see Figure 3 in Zamanov et al. 2017), but it is similar to that of the recurrent nova RS Oph (see Figures 3–5 in Zamanov et al. 2018). In the case of AE Aqr, all the data occupy a well-defined strip. Here, such a strip is not visible, although the observations from each night are placed on a specific position on the diagram. This indicates that the flickering behavior of MWC 560 has a similar mechanism to that of RS Oph but is different than that of AE Aqr.

In Figure 4, we plot the calculated mean values for each night (one night–one point). The error bars correspond to the standard deviation of the run. The left panel is the observed component, and the right panel is the hot component (red giant contribution subtracted). In Figure 4a, it can be seen that the color of the system is in the range $0.31 \leq B - V \leq 0.67$, without a clear tendency to become redder or bluer when the brightness changes.

However, there is a correlation between the mean color and magnitude of the hot component. When we use the 15 points, when the flickering exists, we calculate Pearson correlation coefficient to be 0.91, Spearman's (rho) rank correlation to be 0.88, and the statistical significance

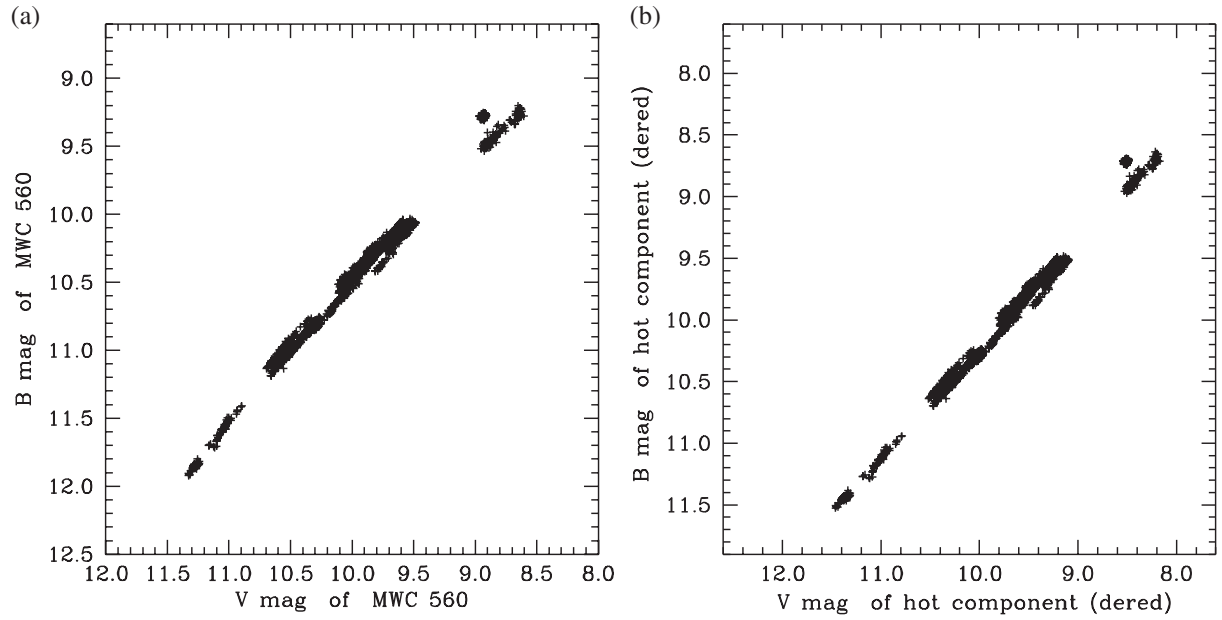

FIGURE 2 B- versus V-band magnitude: (a) observed, (b) calculated for the hot component

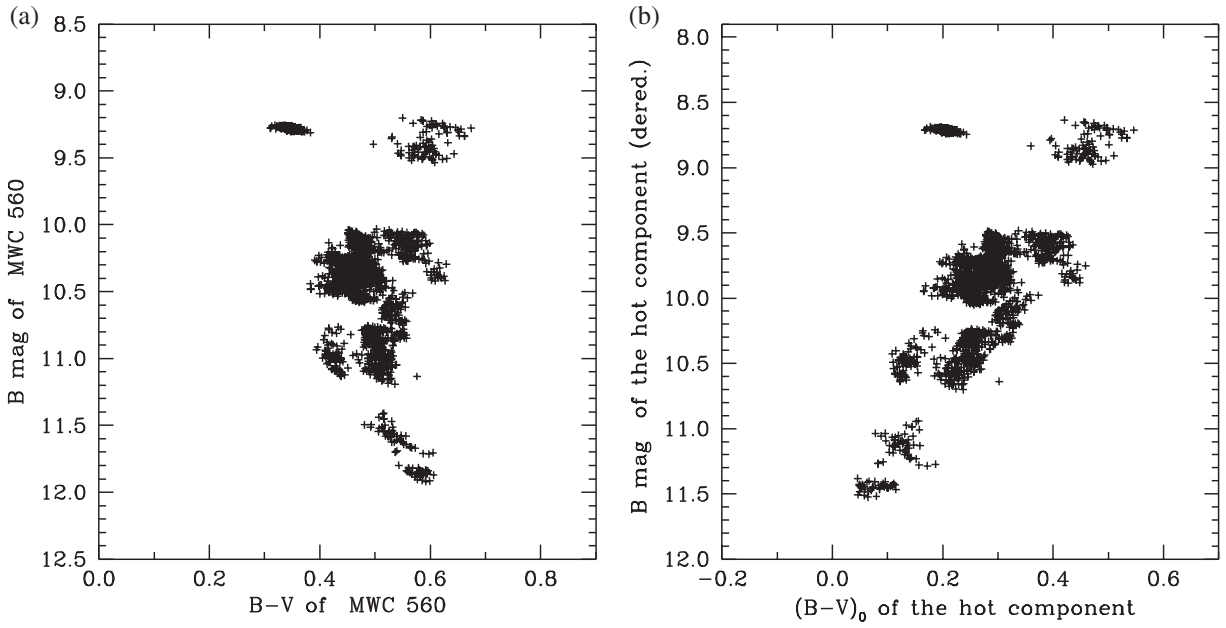

FIGURE 3 Color magnitude diagram: (a) observed, (b) calculated for the hot component

p-value $= 5.9 \times 10^{-5}$. This indicates that the hot component becomes redder as it gets brighter.

When we use all 17 points, including the two nights without flickering, this correlation weakens: Pearson correlation coefficient is 0.58, Spearman's (rho) rank correlation 0.45, and *p-value* = 0.07. This indicates that the missing flickering is connected to the violation of the color–brightness relation of the accretion disc and/or probably changes in its structure/geometry.

5 | FLICKERING LIGHT SOURCE

Bruch (1992) proposed that the light curve of a white dwarf with flickering can be separated into two parts—constant light and variable (flickering) source. Following his formula, we calculate the flux of the flickering light source as $F_{\rm fl1} = F_{\rm av} - F_{\rm min}$, where $F_{\rm av}$ is the average flux during the run, and $F_{\rm min}$ is the minimum flux during the run (corrected for the typical error of the observations).

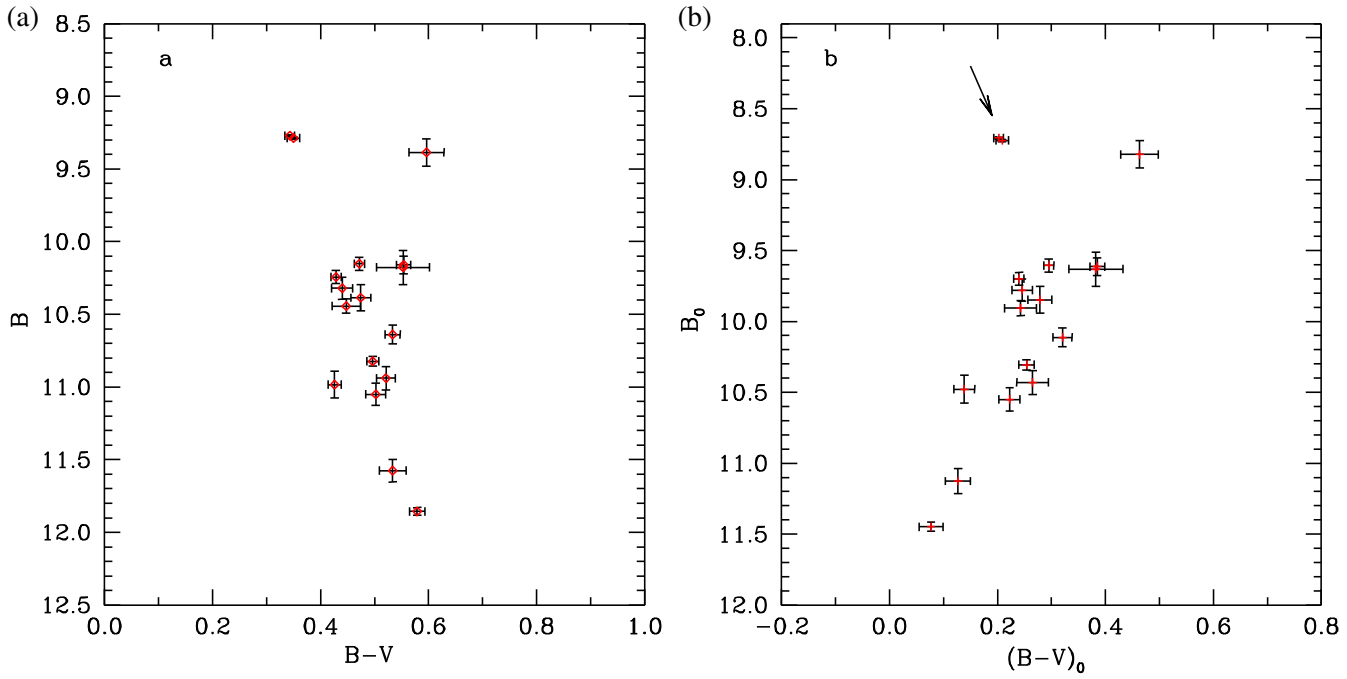

FIGURE 4 Mean color magnitude diagram; each point represents one run: (a) observed, (b) calculated for the hot component; the arrow indicates the two nights without detectable flickering

An expansion of the method is proposed by Nelson et al. (2011). They suggest using $F_{\rm fl2} = F_{\rm max} - F_{\rm min}$, where $F_{\rm max}$ is the maximum flux during the run. In fact, the method of Bruch (1992) evaluates the average brightness of the flickering source, while that of Nelson et al. (2011) evaluates its maximal brightness. $F_{\rm fl1}$ and $F_{\rm fl2}$ have been calculated for each band using the values given in Table 2 and the calibration for a zero-magnitude star $F_0(B) = 6.293\times10^{-9}$ erg cm^{-2} s^{-1} Å^{-1}, $\lambda_{eff}(B) = 4378.12$ Å, $F_0(V) = 3.575\times10^{-9}$ erg cm^{-2} s^{-1} Å^{-1}, and $\lambda_{eff}(V) = 5466.11$ Å as given in the Spanish Virtual Observatory Filter Profile Service (Rodrigo et al. 2018, see also Bessell 1979).

It is worth noting that, while the calculated colors of the hot component depend on the assumed red giant brightness, the parameters of the flickering source are independent of the red giant parameters.

Using the method of Bruch (1992), we find that, in the B-band, the flickering light source contributes about 12% of the average flux of the system, with $0.06 \le F_{\rm fl1}/F_{\rm av} \le 0.20$. In the V-band, its average contribution is 11%, with $0.05 \le F_{\rm fl1}/F_{\rm av} \le 0.17$.

Using the method of Nelson et al. (2011), we find that, in the B-band, the flickering light source contributes about 22% of the maximal flux of the system, with $0.11 \le F_{\rm fl2}/F_{\rm max} \le 0.30$. In the V-band, it is about 21%, with $0.08 \le F_{\rm fl2}/F_{\rm max} \le 0.29$.

From the amplitude–flux relation (rms-flux relation), as given by, for example, Scaringi et al. (2015), we expect that the luminosity of the flickering source will increase as the brightness increases. However, it is not a priori clear which parameter—temperature or radius (or both)—increases.

Table 3 shows the dereddened color of the flickering source $(B-V)_{01}$ and $(B-V)_{02}$; T_1 and T_2, temperature of the flickering source; and R_1 and R_2, radius of the flickering source.

In the given calculations, we assume that the flickering source is continuum-dominated. In principle, it is possible that the flickering involves both continuum and lines. However, the search for rapid spectral variability related to the flickering in MWC 560 shows that there are no changes higher than a few percentage levels in the optical lines in spite of 0.35-mag flickering in the B-band (Tomov et al. 1995). Our simultaneous five-color photometry shows that the flickering source is well approximated with the black body in the UBVRI bands (Zamanov et al. 2011c). The observations of the near-UV flickering show that near-UV spectral morphology remained constant, so the near-UV flickering must have originated in a variable continuum (Lucy et al. 2020). Bearing in mind the above, as well the discussion in Section 6.2 of Sokoloski et al. (2001) about the difficulty of producing rapid variability from the nebular emission, we find that the flickering of MWC 560 is continuum-dominated and reflects the physical origin of the variations in the accretion disc around the white dwarf.

Date		T_1	R_1		T_2	R_2
YYYYMMDD	$(B-V)_{01}$	[K]	[$R_\odot$]	$(B-V)_{02}$	[K]	[$R_\odot$]
20091114	0.1958	9302	1.24	0.0821	11,053	1.28
20100111	0.2400	8750	2.27	0.2461	8674	3.55
20101229	0.3744	7380	5.14	0.2323	8846	5.38
20110210	0.3365	7696	5.94	0.3391	7674	8.41
20110211	0.2604	8495	3.85	0.1952	9310	4.57
20110212	0.2743	8321	4.46	0.2277	8904	5.43
20120321	0.2503	8621	3.25	0.4199	7001	7.92
20120323	0.5001	6499	5.88	0.5325	6297	9.76
20130303	0.3870	7275	3.29	0.4591	6756	5.67
20130305	0.1355	10,082	2.24	0.2348	8815	4.42
20131129	0.1907	9366	2.71	0.2699	8376	5.55
20151118	0.1537	9829	4.50	0.2575	8531	7.65
20160402	0.5379	6263	13.63	0.4870	6581	18.74
20170222	0.4304	6935	6.57	0.3784	7347	8.13
20180124	0.2319	8851	2.64	0.1845	9444	4.13

TABLE 3 The calculated parameters of the flickering source of MWC 560. $(B-V)_{01}$, T_1, and R_1 are dereddened color, temperature, and radius of the flickering source calculated, respectively, following Bruch (1992); $(B-V)_{02}$, T_2, and R_2 following Nelson et al. (2011); see Section 5 for details

5.1 | B–V color and temperature of the flickering source

The calculated dereddened colors of the flickering light source are given in Table 3, where $(B-V)_{01}$ is calculated using $F_{\rm av}$ and $F_{\rm min}$, while $(B-V)_{02}$ is calculated using $F_{\rm max}$ and $F_{\rm min}$. Typical error is ±0.05 mag.

In Figure 5, we plot $(B-V)_{02}$ versus $(B-V)_{01}$. The solid line represents $(B-V)_{02} = (B-V)_{01}$. To check for a systematic shift between the two methods, we performed linear least-squares approximation in one-dimension ($y = a + bx$), where both x and y data have errors. We obtain $a = 0.01 \pm 0.02$ and $b = 0.95 \pm 0.07$. A Kolmogorov–Smirnov test gives Kolmogorov–Smirnov statistic of 0.07 and significance level of 0.99. It means that both methods give similar results, and there is no systematic shift. The average difference between them is ≈0.07 mag, which is comparable with the accuracy of our estimations. In Figure 6, we plot $(B-V)_0$ versus the average B-band magnitude. We do not detect a statistically significant correlation between the color of the flickering source and the brightness of the system.

We calculate the temperature of the flickering source using its dereddened colors and the colors of the black body (Straizys et al. 1976). T_1 is calculated using $(B-V)_{01}$, and T_2 is calculated using $(B-V)_{02}$. The two methods give similar results for the temperature of the flickering source, as well as for $(B-V)_0$. The average values are $T_1 = 8{,}244 \pm 1{,}180$ and $T_2 = 8{,}241 \pm 1{,}290$.

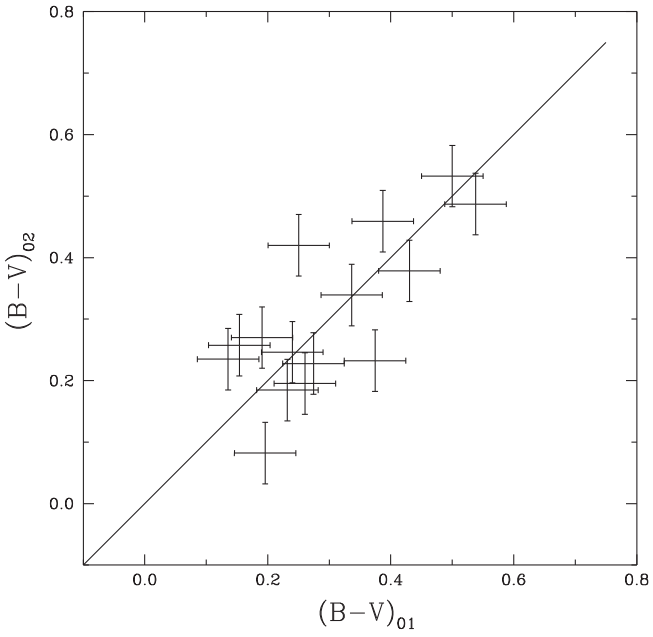

FIGURE 5 $(B-V)_{02}$ versus $(B-V)_{01}$—there is no systematic shift between the two methods. See Section 5.1 for details

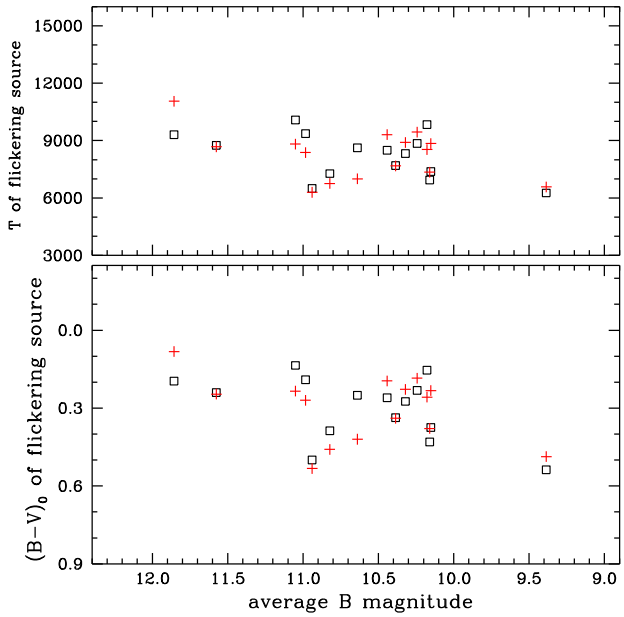

FIGURE 6 Temperature and $(B-V)_0$ color of the flickering source versus the average B magnitude. The squares represent values calculated by method of Bruch (1992), and the plus signs are derived following Nelson et al. (2011)

5.2 | Radius and luminosity of the flickering source

The radius of the flickering source is calculated using the derived temperature (Section 5.1) and the B-band magnitude, assuming that it is spherically symmetric. We obtain $1.2 < R_1 < 13.6\ R_\odot$ and $1.3 < R_2 < 18.7\ R_\odot$. In Figure 7, we plot R_1 and R_2 versus the average B-band magnitude. The radius of the flickering source is observed to increase when the brightness of the system increases.

The luminosity of the flickering source is calculated using the derived temperature and the radius given in Table 3: $L_1 = 4\pi R_1^2 \sigma T_1^4$, where σ is the Stefan-Boltzmann constant. We obtain $10.4\ L_\odot < L_1 < 260\ L_\odot$ and $22\ L_\odot < L_2 < 600\ L_\odot$.

We found a strong correlation between the average B-band magnitude and R_1 with a Pearson correlation coefficient of 0.765, Spearman's (rho) rank correlation of 0.761, and significance $p\text{-}value = 9.9 \times 10^{-4}$. The correlation between B and R_2 is weaker. There are also strong correlations between B and L_1—Pearson 0.785, Spearman 0.782, and $p\text{-}value = 5.7 \times 10^{-4}$—as well as between B and L_2—Pearson 0.79, Spearman's 0.80, and $p\text{-}value = 3.0 \times 10^{-4}$.

6 | DISCUSSION

During the last few decades, MWC 560 underwent three optical brightenings—1990, 2010–2011, and 2016. Multiwavelength observations (including optical, ultraviolet, X-ray, and radio data) in the last few years, as well as a model accounting for the similarities and the differences between the brightening events, are presented by Lucy et al. (2020). The observations of the intranight variability during the 1990 outburst are presented and analyzed in Tomov et al. (1996) and Zamanov et al. (2011b). The current dataset covers the period 2009–2019. The long-term light curve (Doroshenko et al. 1993; Leibowitz & Formiggini 2015) indicates that, during our observations, MWC 560 was, on average, three to four times brighter in the optical bands than before 1989.

Random fluctuations of the brightness are observed throughout diverse classes of objects that accrete material onto a compact object (white dwarf, neutron star, or black hole)—cataclysmic variables, X-ray binaries, and active galactic nuclei. Photoelectric observations identified the flickering as a common characteristic of the accreting white dwarfs in cataclysmic variables (Henize 1949; Mumford 1966; Robinson 1973). The flickering appears as stochastic light variations on timescales of about 10 min with amplitude from a few ×0.01 mag to more than one magnitude. Three different places are considered the source of flickering from accreting white dwarfs—the accretion disc itself, its outer edge (bright spot), and its inner edge (boundary layer).

6.1 | Bright spot

The temperature and the size of the bright spot are derived for a few cataclysmic variables. For OY Car, Wood et al. (1989) calculated temperature in the range 8,600–15,000 K; Zhang & Robinson (1987) for U Gem as $T = 11,600 \pm 500$ K; and Robinson et al. (1978) found $T = 16{,}000$ K for the bright spot in WZ Sge. For IP Peg, three estimates exist: Marsh (1988)—$T = 12{,}000 \pm 1{,}000$ K, Ribeiro et al. (2007)—6000–10,000 K, Copperwheat et al. (2010)—7,000–13,000 K. The temperature of the optical flickering source of MWC 560 is in the range $6{,}200 < T_{fl} < 10{,}100$ K (see Section 4.1), which is similar to the temperature of the bright spot of cataclysmic variable stars.

The bright spot is produced by the impact of the stream on the outer parts of the accretion disc. In case of Roche-lobe overflow, this stream comes from the inner Lagrangian point L_1. If the red giant in MWC 560 does not fill its Roche lobe, the white dwarf accretes material from its wind. In this case accretion cone and accretion wake will be formed, for example, Figure 4 of Ahmad et al. (1983). The stream formed in the accretion wake should be similar to that formed from Roche-lobe overflow. The luminosity of the bright spot is approximately

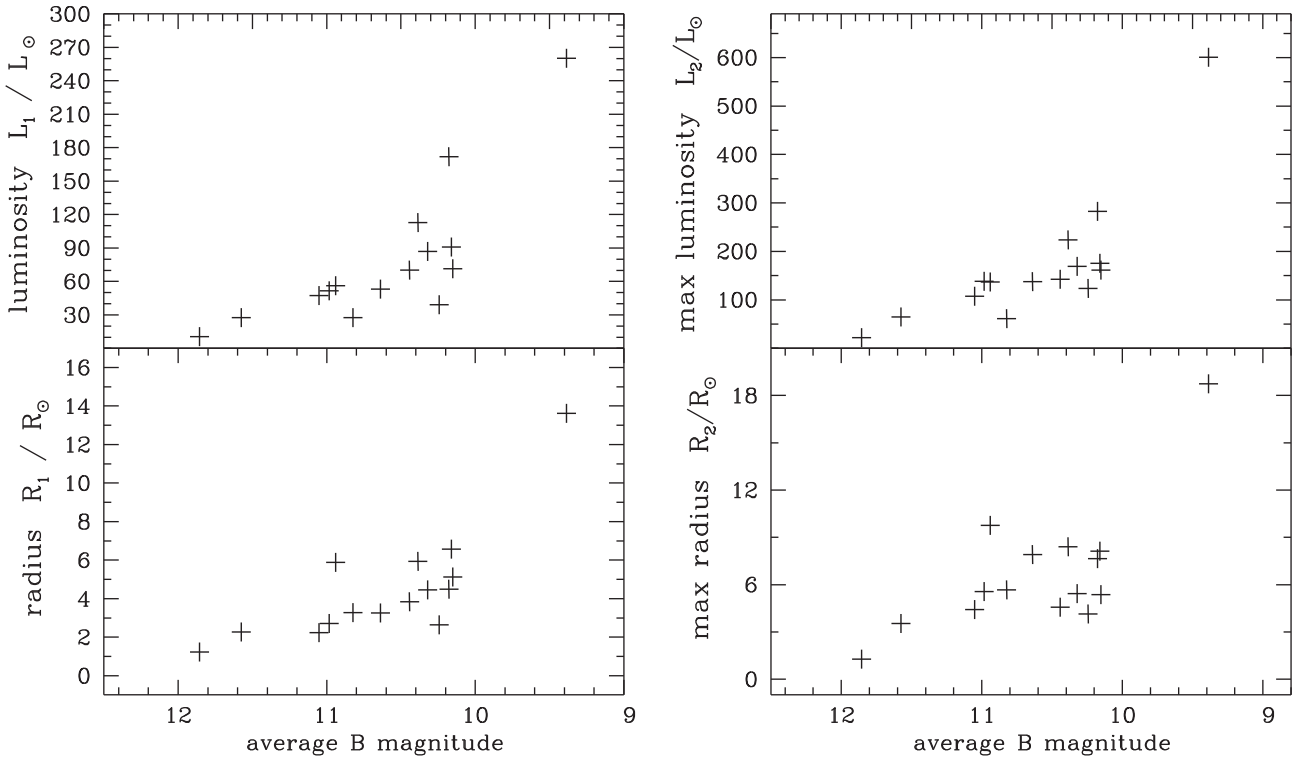

FIGURE 7 Radius and luminosity of the flickering source of MWC 560 versus the average B-band magnitude. The left panels are average L_1 and R_1; the right are the maximum L_2 and R_2 (see Section 5)

(Elsworth & James 1982; Shu 1976):

$$L_{bs} \approx \frac{1}{2}\ V_{\perp}^{2}\ \dot{M}_{acc}, \tag{1}$$

where $\dot{M}_{acc}$ is the mass accretion rate, and $V_{\perp}$ is the inward component of the stream's velocity at the impact with the disc. Equation (1) indicates that, when the mass accretion rate increases, the luminosity of the spot must also increase. In addition, our results (Section 5.2) indicate that, when the mass accretion rate increases, the radius of the bright spot (if it is the source of flickering) also increases, while its temperature remains almost constant.

6.2 | Temperature in the accretion disc

The broadband variability is often attributed to (a) inward propagating fluctuations driven by stochastic variability in the angular momentum transport mechanism (Lyubarskii 1997), (b) turbulence and vortexes in the disc (Dobrotka et al. 2010; Kurbatov & Bisikalo 2017), and (c) spiral structures in the disc (Baptista & Bortoletto 2008). The timescales of changes of the overall structure of the accretion disc are longer compared to the local fluctuating processes in the flow that can generate the flickering. In this way, the dynamical timescale variability of the flickering light source does not change the overall structure of the accretion disc. Considering the entire disc structure, the temperature in the disc can be approximated with the radial temperature profile of a steady-state accretion disc (Frank et al. 2002):

$$T_{eff}^{4} = \frac{3G\dot{M}_{acc}M_{wd}}{8\pi\sigma R^{3}}\left[1-\left(\frac{R_{wd}}{R}\right)^{1/2}\right], \tag{2}$$

R is the radial distance from the white dwarf. We assume $M_{wd} = 0.9\ M_{\odot}$ and $R_{wd} = 6\times10^{8}$ cm (Lucy et al. 2020; Zamanov et al. 2011a) and a mass accretion rate of about $5\times10^{-7}\ M_{\odot}$ year^{-1} (Schmid et al. 2001).

Using the parameters for MWC 560, a temperature $6{,}300 \le T_{fl} \le 10{,}000$ K (the temperature of the flickering light source as given in Table 3) should be achieved at a distance $R \approx 1.2 - 2.5\ R_{\odot}$ from the white dwarf. If the accretion disc itself is the place of origin of the flickering of MWC 560, then it comes at a distance $R \sim 2\ R_{\odot}$ from the white dwarf.

6.3 | Boundary layer

The boundary layer between the white dwarf and the inner edge of the accretion disc should have a temperature $\geq 10^{5}$ K (Mukai 2017). The derived temperature of the flickering source is considerably lower than that expected from the

boundary layer. If the boundary layer is optically thick, in this case, the radius of the flickering source measured in the optical bands (Figure 7) could represent the radius up to which the emission generated from the boundary layer is reprocessed by the inner parts of the accretion disc and the accretion disc corona.

6.4 | Disappearance of the flickering

The first indication that the flickering of symbiotic stars sometimes disappears was found for the recurrent nova T CrB (Bianchini & Middleditch 1976). In CH Cyg, the flickering was missing for more than 3 years (Stoyanov et al. 2018). In RS Oph, the flickering disappeared after the nova outburst and reappeared 241 days later (Worters et al. 2007). In MWC 560, the flickering was visible in all observations obtained between 1984 and May 2018 (Lucy et al. 2020; Tomov et al. 1996; Zamanov et al. 2011b, 2011c). It disappeared in October 2018 (Goranskij et al. 2018) and is not visible in our observations obtained in October 2019 and February 2020. The following could be reasons for disappearance of the flickering:

1. If the source of the flickering is a bright spot, then it means that, for some reason, $V_{\perp} \approx 0$ (see Equation (1)). In other words, at the impact point, the stream has velocity approximately equal to the velocity of the outer disc edge.
2. If the source of the flickering is the accretion disc, the disappearance means that the stochastic fluctuations disappear, and the disc becomes stable (nonfluctuating).
3. Goranskij et al. (2018) proposed that a common envelope is formed due to the transit of the system to a dynamical mode of accretion with an increased rate. The accretion matter filling the Roche lobe of the compact companion blocked the jets and overlapped the direct visibility of the companion, so flickering was deleted.

In MWC 560, at the disappearance of the flickering, the hot component becomes bluer, but its brightness in the B-band remains high (see Figure 4b, where the arrow indicates the observations without flickering). This could be an indication that the accretion disc becomes smaller and/or hotter.

In X-rays, MWC 560 is of β/δ type, that is, with two X-ray thermal components—soft and hard (Luna et al. 2013). The soft emission is most likely produced in a colliding-wind region, and the hard emission is most likely produced in a boundary layer between accretion disc and white dwarf. The changes in the X-ray emission can give us clues why the flickering disappeared.

7 | CONCLUSIONS

We report quasisimultaneous observations of the flickering variability of the jet-ejecting symbiotic star MWC 560 for 17 nights during the period November 2011 to October 2019. The color-magnitude diagram, B versus B–V, shows that, when the flickering exists, the hot component of the system becomes redder as it gets brighter.

For the flickering source, we find that it has color in the range $0.14 < B-V < 0.40$, temperature in the range $6{,}300-11{,}000$ K, and radius in the range $1.2-18\ R_{\odot}$. The estimated temperature is similar to that of the bright spot of cataclysmic variables. We do not find a correlation between the temperature of the flickering and the brightness. However, we do find strong correlations (a) between B-band magnitude and the average radius of the flickering source—as the brightness of the system increases, the size of the flickering source also increases, and (b) between B-band magnitude and the luminosity of the flickering source—as the brightness of the system increases, the luminosity of the flickering source also increases. When the flickering disappeared in 2019, the B–V color of the hot component became bluer, but its brightness in UBV remained high.

The behavior of the hot component and flickering source in MWC 560 should provide useful input for the theoretical modeling of accretion in symbiotic-type binaries.

ACKNOWLEDGMENTS

We dedicate this paper to the memory of Prof Toma Tomov (1953–2019), who initiated the observations of MWC 560 at Rozhen Observatory. This work was supported by the grant KP-6-H28/2"Binary stars with compact object" (Bulgarian National Science Fund).

REFERENCES

Ahmad, I. A., Chapman, R. D., & Kondo, Y. 1983, *A&A*, *126*, L5.
Angeloni, R., Di Mille, F., Lopes, C. E. F., & Masetti, N. 2013, *IAUS*, *179*, 290.
Baptista, R., & Bortoletto, A. 2008, *ApJ*, *676*, 1240.
Bessell, M. S. 1979, *PASP*, *91*, 589.
Bianchini, A., & Middleditch, J. 1976, *IBVS*, *1151*, 1.
Bond, H. E., Pier, J., Pilachowski, C., Slovak, M., & Szkody, P. 1984, *BAAS*, *16*, 516.
Bonev, T., & Dimitrov, D. 2010, *BlgAJ*, *13*, 153.
Bruch, A. 1992, *A&A*, *266*, 237.
Copperwheat, C. M., Marsh, T. R., Dhillon, V. S., Littlefair, S. P., Hickman, R., Gänsicke, B. T., & Southworth, J. 2010, *MNRAS*, *402*, 1824.

Dobrotka, A., Hric, L., Casares, J., Shahbaz, T., Martínez-Pais, I. G., & Muñoz-Darias, T. 2010, *MNRAS*, *402*, 2567.
Dobrzycka, D., Kenyon, S. J., & Milone, A. A. E. 1996, *AJ*, *111*, 414.
Doroshenko, V. T., Goranskij, V. P., & Efimov, Y. S. 1993, *IBVS*, *3824*, 1.
Elsworth, Y. P., & James, J. F. 1982, *MNRAS*, *198*, 889.
Frank, J., King, A., & Raine, D. J. 2002, *Accretion Power in Astrophysics*, 3rd ed. Cambridge: Cambridge University Press.
Gaia Collaboration, Brown, A. G. A., Vallenari, A., et al. 2018, *A&A*, *616*, 1.
Goranskij, V. P., Zharova, A. V., Barsukova, E. A., & Burenkov, A. N. 2018, *ATel*, *12227*, 1.
Gromadzki, M., Mikolajewski, M., Tomov, T., Bellas-Velidis, I., Dapergolas, A., & Galan, C. 2006, *AcA*, *56*, 97.
Gromadzki, M., Mikołajewska, J., Whitelock, P. A., & Marang, F. 2007, *A&A*, *463*, 703.
Henden, A., & Munari, U. 2006, *A&A*, *458*, 339.
Henize, K. G. 1949, *AJ*, *54*, 89.
Houdashelt, M. L., Wyse, R. F. G., & Gilmore, G. 2001, *PASP*, *113*, 49.
Koornneef, J. 1983, *A&A*, *500*, 247.
Kurbatov, E. P., & Bisikalo, D. V. 2017, *ARep*, *61*, 475.
Leibowitz, E. M., & Formiggini, L. 2015, *AJ*, *150*, 52.
Lucy, A. B., Knigge, C., & Sokoloski, J. L. 2018, *MNRAS*, *478*, 568.
Lucy, A. B., Sokoloski, J. L., Munari, U., et al. 2020, *MNRAS*, *492*, 3107.
Luna, G. J. M., Sokoloski, J. L., Mukai, K., & Nelson, T. 2013, *A&A*, *559*, A6.
Lyubarskii, Y. E. 1997, *MNRAS*, *292*, 679.
Marsh, T. R. 1988, *MNRAS*, *231*, 1117.
Merrill, P. W., & Burwell, C. G. 1943, *ApJ*, *98*, 153.
Mikołajewska, J. 2012, *BaltA*, *21*, 5.
Mukai, K. 2017, *PASP*, *129*, 062001.
Mumford, G. S. 1966, *ApJ*, *146*, 411.
Munari, U., Dallaporta, S., Castellani, F., et al. 2016, *NewA*, *49*, 43.
Nelson, T., Mukai, K., Orio, M., Luna, G. J. M., & Sokoloski, J. L. 2011, *ApJ*, *737*, 7.
Ribeiro, T., Baptista, R., Harlaftis, E. T., Dhillon, V. S., & Rutten, R. G. M. 2007, *A&A*, *474*, 213.
Robinson, E. L. 1973, *ApJ*, *183*, 193.
Robinson, E. L., Nather, R. E., & Patterson, J. 1978, *ApJ*, *219*, 168.
Rodrigo, C., Solano, E., Bayo, A. 2018, The SVO Filter Profile Service, Available at: http://ivoa.net/documents/Notes/SVOFPS/index.html.
Savage, B. D., & Mathis, J. S. 1979, *ARA&A*, *17*, 73.
Scaringi, S., Maccarone, T. J., Körding, E., et al. 2015, *SciA*, *1*, e1500686.
Schmid, H. M., Kaufer, A., Camenzind, M., et al. 2001, *A&A*, *377*, 206.
Shu, F. H. 1976, *IAU Symposium*, *73*, 253.
Sokoloski, J. L., Bildsten, L., & Ho, W. C. G. 2001, *MNRAS*, *326*, 553.
Stoyanov, K. A., et al. 2018, *BlgAJ*, *28*, 42.
Straizys, V., Sudzius, J., & Kuriliene, G. 1976, *A&A*, *50*, 413.
Strigachev, A., & Bachev, R. 2011, *BlgAJ*, *16*, 144.
Szkody, P., Mateo, M., & Schmeer, P. 1990, *IAUC*, *4987*, 1.
Tody, D. 1993, *ASPC*, *173*, 52.
Tomov, T., Kolev, D., Georgiev, L., Zamanov, R., Antov, A., & Bellas, Y. 1990, *Natur*, *346*, 637.
Tomov, T., Kolev, D., Munari, U., Sostero, G., & Lepardo, A. 1995, *A&A*, *300*, 769.
Tomov, T., Kolev, D., Ivanov, M., et al. 1996, *A&AS*, *116*, 1.
Wood, J. H., Horne, K., Berriman, G., & Wade, R. A. 1989, *ApJ*, *341*, 974.
Worters, H. L., Eyres, S. P. S., Bromage, G. E., & Osborne, J. P. 2007, *MNRAS*, *379*, 1557.
Zamanov, R., & Marziani, P. 2002, *ApJL*, *571*, L77.
Zamanov, R., Gomboc, A., & Latev, G. 2011a, *BlgAJ*, *16*, 18.
Zamanov, R. K., Tomov, T., Bode, M. F., Mikołajewski, M., Stoyanov, K. A., & Stanishev, V. 2011b, *BlgAJ*, *16*, 3.
Zamanov, R., Boeva, S., Latev, G., Stoyanov, K., Bode, M. F., Antov, A., & Bachev, R. 2011c, *IBVS*, *5995*, 1.
Zamanov, R. K., Latev, G. Y., Boeva, S., Ibryamov, S., Nikolov, G. B., & Stoyanov, K. A. 2017, *AN*, *338*, 598.
Zamanov, R. K., Boeva, S., Latev, G. Y., et al. 2018, *MNRAS*, *480*, 1363.
Zhang, E.-H., & Robinson, E. L. 1987, *ApJ*, *321*, 813.
Zhekov, S. A., Hunt, L. K., Tomov, T., & Gennari, S. 1996, *A&A*, *309*, 800.

AUTHOR BIOGRAPHY

R. K. Zamanov, born on 17.11.1964 Graduated in Sofia University St. Kl. Ohridski (1989) PhD - Bulgarian Academy of Sciences (1997) Postdoc - Padova, Italy (2001-2003) postdoc research assistant - Liverpool John Moores University, UK (2003-2005) proffesor of astrophysics and stellar astronomy - Sofia, Bulgaria (since 2012).

How to cite this article: Zamanov RK, Boeva S, Stoyanov KA, et al. Flickering of the jet-ejecting symbiotic star MWC 560. *Astron. Nachr.*. 2020;1–11. https://doi.org/10.1002/asna.202013730